Research Square

Preprints are preliminary reports that have not undergone peer review.
They should not be considered conclusive, used to inform clinical practice,
or referenced by the media as validated information.

Development, optimization, and functional characterization of a gelatin-based hydrogel biodegradable packaging film for sustainable food packaging and refrigerated cherry tomato preservation

Navneeta Deogharia
D.Y. Patil University
Rashi Gurav
D.Y. Patil University
Harsh Priyadarshi
D.Y. Patil University
Mansi Singh
D.Y. Patil University
Pankaj B Pathare
Sultan Qaboos University
Pratik S Gaikwad
pratik.gaikwad@dypatil.edu

D.Y. Patil University

Research Article

Keywords: Gelatin-based hydrogel film, active biodegradable packaging, cherry tomatoes, refrigerated storage, shelf life extension

Posted Date: November 13th, 2026

DOI: https://doi.org/10.21203/rs.3.rs-11295202/v1

License: This work is licensed under a Creative Commons Attribution 4.0 International License.
Read Full License

Additional Declarations: No competing interests reported.

Development, optimization, and functional characterization of a gelatin-based hydrogel biodegradable packaging film for sustainable food packaging and refrigerated cherry tomato preservation

Navneeta Deogharia,[a] Rashi Gurav,[a] Harsh Priyadarshi,[a] Mansi S. Singh,[a] Pankaj B. Pathare*[b] and Pratik S. Gaikwad*[a]

0000-0001-5140-0272*[b] and 0000-0003-2373-4392*[a]

[a]School of Biotechnology & Bioinformatics, D Y Patil (Deemed to be University), Navi Mumbai, Maharashtra, India

[b]Department of Soils, Water and Agricultural Engineering, College of Agricultural & Marine Sciences, Sultan Qaboos University, Oman

***Corresponding author's details**

[a]Dr. Pratik Subhash Gaikwad, Ph.D.
Assistant Professor,
School of Biotechnology & Bioinformatics,
D Y Patil (Deemed to be University),
Navi Mumbai – 400614, Maharashtra, India.
E-mail ID: pratik.gaikwad@dypatil.edu
ORCID: 0000-0003-2373-4392
Contact No: +91-9920942607

[b]Dr. Pankaj B. Pathare,
Assistant Professor,
Department of Soils, Water and Agricultural Engineering,
College of Agricultural & Marine Sciences, Sultan Qaboos University, Oman.
E-mail ID: pankaj@squ.edu.om
ORCID: 0000-0001-5140-0272
Contact No: +968 9638 0899

Abstract

This study aimed to develop and characterize gelatin-based hydrogel active biodegradable packaging films formulated using the solvent casting method. Three formulations (S1-S3 films) were evaluated for physicochemical, thermal, and functional properties. FTIR spectra revealed characteristic O–H/N–H (3302–3303 cm^{-1}), C–H (2924–2930 cm^{-1}), and amide I–II (1642–1550 cm^{-1}) peaks, confirming intermolecular hydrogen bonding and composite matrix formation. Mechanical testing showed that tensile strength decreased from 0.203 ± 0.012 MPa (S1 film) to 0.091 ± 0.013 MPa (S3 film), while elongation ranged from 248.9 ± 4.33 % to 189.07 ± 3.68 %. Barrier studies indicated that WVTR reduced from 54.10 ± 1.51 to 46.06 ± 1.16 $g \cdot m^{-2} \cdot day^{-1}$ and OTR from 210 ± 4.08 to 181.67 ± 6.24 $cm^3 \cdot m^{-2} \cdot day^{-1} \cdot atm^{-1}$ with increasing gelatin concentration. DSC analysis exhibited dual glass transitions (Tg_1 = 39.09 °C; Tg_2 = 51.92 °C) and a melting point at 188.7 °C (ΔHm = 156.48 $J \cdot g^{-1}$), indicating semi-crystalline stability. FE-SEM revealed a compact porous network (3.9–8.9 µm), while Total Plate Count remained <10 CFU/mL after 30 days. Soil burial tests confirmed > 95 % biodegradation within 15 days, validating the film's environmental compatibility for active and sustainable food packaging applications. The selected S2 gelatin-based hydrogel film was evaluated for packaging cherry tomatoes under refrigerated storage at 4 ± 1 °C. Visible surface shrinkage was first observed on day 12 in the control and on day 15 in the S2 hydrogel-film packaged cherry tomatoes, indicating a 3-day extension in apparent visual shelf life.

Keywords

Gelatin-based hydrogel film; active biodegradable packaging; cherry tomatoes; refrigerated storage; shelf life extension.

Highlights

1. Gelatin-based active biodegradable hydrogel films were developed by solvent casting.
2. S2 gelatin-based hydrogel film showed most balanced mechanical and barrier properties.
3. The selected S2 film showed dual glass transitions and good thermal stability.
4. The selected S2 film achieved more than 95% biodegradation within 15 days.
5. Selected S2 film delayed visible cherry tomato surface shrinkage by 3 days at 4 ± 1 °C.

1. Introduction

Growing awareness of food safety, environmental protection, and the need to reduce global waste has accelerated efforts to discover new food packaging systems. Although conventional plastic packaging provides effective protection and extended shelf life, its non-biodegradable nature results in long-term ecological accumulation that threatens land and marine environments [1,2]. These concerns have encouraged the development of sustainable materials that preserve food while lowering environmental impact.

Food spoilage remains a critical issue worldwide, causing major losses in food quality, nutritional value, and market availability. Spoilage commonly arises due to microbial contamination, oxidative reactions, and uncontrolled moisture transfer [3,4]. Foodborne pathogens, including *Escherichia coli*, *Salmonella* spp., and *Listeria monocytogenes*, lead to undesirable sensory changes such as altered texture, unpleasant odors, and off-flavors, making food unsuitable for consumption [5]. Oxidation of fats, proteins, and oils also plays a central role in quality deterioration, particularly in meat, dairy, and fat-rich snacks, where breakdown of nutrients and aroma compounds affects consumer acceptance [4,6,7]. Similarly, unregulated moisture results in wilting, softening, or hardening of foods such as fruits and vegetables, compromising freshness and visual appeal [6,8]. These challenges demonstrate the need for packaging technologies that can control microbial growth, slow oxidative processes, and regulate moisture.

Biodegradable materials developed from renewable biological sources present strong potential as substitutes for petroleum-based plastics. Hydrogels are one such material and consist of water-holding three-dimensional (3D) polymer networks formed from natural or synthetic biopolymers [9]. Their ability to absorb and retain water, respond to environmental triggers, and carry functional compounds has positioned them as promising platforms for food packaging applications [10,11]. The modification of hydrogel matrices with natural compounds allows the incorporation of antimicrobial and antioxidant activity. These properties can help slow spoilage, maintain quality, and enhance product safety without introducing toxic residues [9,12].

Hydrogel-based active packaging also supports global sustainability goals because it uses renewable materials, promotes resource recovery, and minimizes long-term waste accumulation [13]. Along with serving as a physical barrier, these materials can regulate moisture and control the release of bioactive compounds, enabling them to actively preserve

food rather than merely contain it [11,14]. Therefore, hydrogel systems provide an opportunity to replace traditional plastic packaging while supporting environmental safety and public health.

The objective of this study is to develop and optimize biodegradable gelatin-based hydrogel active packaging films using natural polymers and functional additives, and to evaluate their physical, mechanical, and barrier properties, along with their effectiveness in maintaining freshness and extending the shelf life of perishable food products, as a sustainable alternative to conventional plastic packaging.

The objective of this study was to develop and optimize biodegradable gelatin-based hydrogel active packaging films and evaluate their physicochemical, mechanical, barrier, thermal, morphological, microbial, and biodegradation properties. The best-performing formulation was selected for cherry tomato packaging under refrigerated storage at 4 ± 1 °C, with hydrogel-film packaged cherry tomatoes stored in transparent polyethylene terephthalate (PET) clamshell containers and control cherry tomatoes placed directly in identical PET containers without the hydrogel film.

2. Materials and methods

2.1 Procurements of raw materials and chemicals

The materials used for gelatin-based hydrogel formulation and subsequent analysis were procured from dependable commercial sources to ensure quality and reproducibility. All ingredients involved in the preparation of the gelatin-based hydrogel matrix were obtained in food grade quality. “Puremate” veg gelatin was purchased from the local market and served as the primary biopolymer. Neem oil sold under the brand name “Neem Veda” was procured from a local supplier and was used as a natural active ingredient to enhance preservative and functional attributes. Soy lecithin from the brand “Bake King” was obtained through an online platform and functioned as a natural phospholipid emulsifier for stable incorporation of neem oil into the aqueous gelatin phase. These ingredients were selected for their safety profile and suitability for food related applications.

All reagents required for physicochemical, structural, and functional analyses including plasticizers, solvents, and laboratory chemicals were procured from Merck (Sigma, Mumbai, Maharashtra, India) were of analytical reagent (AR) grade and were used without further purification to ensure accuracy and consistency in all analytical procedures. Food grade raw materials were used for gelatin-based hydrogel fabrication while analytical grade chemicals

were reserved for characterization studies. The procurement approach focused on quality, purity, and compliance with research standards for both material preparation and subsequent evaluations.

2.2 Preparation of gelatin-based hydrogel film formulations

The gelatin-based hydrogel formulations were developed in three different concentrations as described in **Table 1**, and each batch was prepared following an identical protocol to maintain experimental consistency.

The preparation began with the formation of the aqueous phase, in which distilled water, gelatin and glycerol were transferred into a borosilicate beaker and heated to 60 ± 1 °C under continuous magnetic stirring. This step facilitated complete hydration and dissolution of the biopolymer, resulting in a clear and uniform gelatin solution. Concurrently, the oil phase was prepared by combining neem oil and soy lecithin in a separate beaker maintained at 60 ± 1 °C with continuous stirring to ensure proper dispersion of the emulsifier within the hydrophobic medium [15].

Following the preparation of both phases, the aqueous phase was introduced dropwise into the oil phase while maintaining vigorous stirring. The controlled addition and high shear conditions promoted the formation of a fine and stable oil in water emulsion, ensuring homogeneous incorporation of neem oil within the biopolymer matrix. The resulting emulsion was subsequently cooled to 40 °C, at which point the crosslinking agent was added to facilitate intermolecular interactions and strengthen the structural integrity of the developing gelatin-based hydrogel network [15].

The prepared gelatin-based hydrogel emulsion was subsequently cast onto a clean, leveled glass surface using the solvent casting method. Casting volume and spreading were carefully controlled to achieve uniform film formation. After drying at 45±1 °C for 48±2 hrs, the films were gently peeled from the casting surface and conditioned in a desiccator [16].

The developed gelatin-based hydrogel films exhibited an average thickness of 75 ± 1 µm, measured in accordance with ASTM D6988 using a digital micrometer (Mitutoyo Digital Micrometer, Model MDC-25MX, Mitutoyo Corp., Kawasaki, Japan). Thickness was measured at five positions, including the center and the four corners, to ensure uniformity across each sample [17].

The finalized gelatin-based hydrogel films were characterized for their functional, mechanical, barrier, thermal, structural, antimicrobial, and biodegradability properties using

the analytical methods described in the subsequent sections. The formulations were comparatively evaluated based on their measured characteristics, and the most suitable formulation was selected for the food packaging application.

2.3 Application of developed suitable gelatin-based hydrogel film for cherry tomato storage

Fresh cherry tomatoes were purchased from the APMC Market, Vashi, Navi Mumbai, Maharashtra 400703, India, and chosen for uniform size and appearance. Tomatoes with visible bruises, cracks, fungal growth, and physical damage were excluded. The selected tomatoes were transported approximately 11 km to the School of Biotechnology & Bioinformatics, D Y Patil (Deemed to be University), CBD Belapur, Navi Mumbai, Maharashtra 400614, India. On arrival, the tomatoes were cleaned to remove adhering dirt and foreign matter, washed thoroughly with clean water, and allowed to drain.

Following comparative characterization of the developed gelatin-based hydrogel film formulations, the formulation with the most suitable combined performance was selected for the packaging fresh cherry tomatoes. The washed tomatoes were packaged using the selected hydrogel film and placed in transparent PET clamshell containers. Control tomatoes were placed directly into transparent PET clamshell containers without the hydrogel film. Both treatments were stored under refrigerated conditions at 4 ± 1 °C (**Fig. 1**).

During storage, samples were visually assessed for changes in external appearance, with particular focus on the development of visible surface shrinkage. The onset of surface shrinkage served as the visual indicator of noticeable quality deterioration, and the apparent shelf life of hydrogel-film packaged tomatoes was compared with that of the control.

2.4 Film characterization

2.4.1 Identification of functional group for developed gelatin-based hydrogel films

Functional group interactions in the gelatin-based hydrogel films were analysed using an Attenuated Total Reflectance–Fourier Transform Infrared (ATR-FTIR) spectrometer (Spectrum Two, PerkinElmer, USA). Film samples were equilibrated for 24 hrs before testing. Spectra were recorded in the range of 4000 to 400 cm^{-1} with a resolution of 4 cm^{-1} and 12 scans per sample. Background correction was performed before each run. The obtained spectra were subsequently baseline corrected and analysed to identify characteristic absorption bands corresponding to the functional groups present in the hydrogel matrix and to assess potential molecular interactions among the constituent components. The characteristic peak positions of

the S1, S2 and S3 formulations were comparatively evaluated, and the wavenumber variation (Δν) for corresponding absorption bands was calculated using Eq. 1, as the difference between the highest and lowest wavenumber recorded among the three formulations. The resulting spectral shifts were used to compare formulation-dependent variations in the vibrational environment of the identified functional groups [18].

$$\Delta v = v_{max} - v_{min} \qquad (1)$$

2.4.2 Mechanical properties of developed gelatin-based hydrogel films

Tensile strength (TS) and elongation at break (% EB) were measured using a Universal Testing Machine (UTM Tinius Olsen 50ST) in accordance with ASTM D882. Film strips of 80 × 10 mm were conditioned for 48 hrs at 23 ± 2 °C and 50 ± 5 % relative humidity (RH). Tests were conducted at a crosshead speed of 50 mm/min. Tensile strength was calculated by dividing the maximum load in Newtons (N) by the cross sectional area (mm^2), and elongation at break was recorded directly to assess film flexibility and ductility [19].

2.4.3 Barrier properties of developed gelatin-based hydrogel films

Water vapour transmission rate (WVTR) was determined according to ASTM F1249 using an infrared sensor based WVTR analyzer (Mocon Permatran-W) operated at 23 ± 2 °C and 50 ± 5% RH. Each gelatin-based hydrogel film was mounted in the test cell separating the dry and humid chambers, and the instrument automatically recorded moisture transmission through the film [20]. WVTR values were expressed in $g \cdot m^{-2} \cdot day^{-1}$, and all measurements were performed in triplicate and reported as mean ± standard deviation (SD).

Oxygen transmission rate (OTR) was measured according to ASTM D3985 using a coulometric oxygen transmission analyzer (Mocon Ox-Tran) under the same controlled conditions of 23 ± 2 °C and 50 ± 5% RH, where each film was sealed in the test cell and oxygen was supplied on one side and nitrogen on the other. The coulometric sensor quantified oxygen permeation through the film, and OTR values were expressed in $cm^3 \cdot m^{-2} \cdot day^{-1} \cdot atm^{-1}$. All OTR measurements were also conducted in triplicate and reported as mean ± SD.

2.4.4 Thermal analysis of selected gelatin-based hydrogel film

Thermal properties of the selected gelatin-based hydrogel film was analysed using a PerkinElmer Differential Scanning Calorimetry (DSC) 6000 (-40 to 400 °C). Film sample weighing 5-10 mg were hermetically sealed in aluminium pans, with an empty pan as reference. Measurements were performed under a nitrogen purge of 20-30 mL/min. Heating scans were

conducted at 10 °C/min. Data were processed using Pyris v5.42 software to determine glass transition (Tg), melting (Tm) and crystallization (Tc) temperatures and enthalpy (ΔHm), which provided insights into molecular interactions, crystallinity, and thermal stability [21].

2.4.5 Surface morphological analysis of selected gelatin-based hydrogel film

Surface morphological analysis of the selected gelatin-based hydrogel film was performed using a Field Emission Scanning Electron Microscopy (FE-SEM TESCAN Viga 3, Kohoutovice, Czech Republic). Film sections of approximately 20 × 20 mm were mounted on aluminium stubs using conductive carbon tape and sputter coated with a thin gold-palladium layer (~100 Å) for 30 sec to minimise charging. Imaging was carried out at an accelerating voltage of 20 kV with magnifications of 100X and 1,200X to evaluate the surface texture, uniformity, and morphological features of the gelatin-based hydrogel film [22].

2.4.6 Total plate count (TPC) of selected gelatin-based hydrogel film

The TPC of the selected gelatin-based hydrogel film was determined following ISO 4833-1:2013 with minor modifications. Microbial load was assessed at 15-day intervals up to 30 days. Film samples were aseptically transferred to sterile saline, vortex-homogenized, serially diluted, and plated on plate count agar. Plates were incubated at 37 °C for 24-48 hrs, and colony counts were expressed as CFU/mL to evaluate changes in microbial load of the selected gelatin-based hydrogel film over time.

2.4.7 Biodegradability test for selected gelatin-based hydrogel film

The biodegradability of the selected gelatin-based hydrogel film was evaluated using the soil burial method in accordance with ASTM D5988. Film specimens measuring 5 × 5 cm were buried at a depth of 10 cm in loamy soil maintained at 60% moisture and 25 ± 2 °C under aerobic conditions [23]. The samples were retrieved at 3-day intervals until complete degradation was achieved.

2.5 Visual shelf life assessment of cherry tomatoes under refrigerated storage

The packaged and control cherry tomatoes were stored at 4 ± 1 °C and visually evaluated at 3-day intervals. At each observation interval, changes in the external appearance of the samples were recorded, with particular attention to visible surface shrinkage as the first indication of noticeable quality deterioration. Photographs were captured using an iPhone 15 Plus camera at 1.5X zoom. The samples were placed on a clean white paper sheet, and the camera was positioned vertically above the samples at a distance of 40 ± 2 cm. The samples were uniformly

illuminated during image acquisition, and the camera distance, vertical orientation, framing, and imaging conditions were maintained consistently throughout the storage study. The photographic records were used to document changes in the external appearance of the tomatoes and identify the first occurrence of visible surface shrinkage. The apparent shelf life was determined based on the onset of visible surface shrinkage and compared between the tomatoes packaged with the selected gelatin-based hydrogel film and the control tomatoes stored directly in transparent PET clamshell containers without the hydrogel film.

2.6 Statistical analysis

The mechanical and barrier properties of the developed gelatin based hydrogel films were statistically evaluated using one way ANOVA followed by Tukey's HSD test in SPSS version 26.0 (SPSS Inc., IL, USA, 2026) to identify significant differences among the samples at a confidence level of $p < 0.05$. All analyses were conducted in triplicate, and the results were expressed as mean ± SD, calculated using Microsoft Excel 2022 (Microsoft Corporation, Redmond, WA, USA).

3. Results and discussion

3.1 Detection of functional group in developed gelatin-based hydrogel films using FTIR spectroscopy

FTIR spectroscopy was used to evaluate functional group interactions and structural differences among the three gelatin-based hydrogel formulations (S1, S2, and S3 films). All films exhibited characteristic absorption bands corresponding to hydroxyl groups, protein amide structures, lipid components, and polysaccharide-derived functionalities, confirming the formation of composite hydrogel matrices. However, notable variations in peak intensity and band assignments were observed, reflecting formulation-dependent molecular interactions. **Table 2** presents the detailed spectral assignments for each gelatin-based hydrogel film formulation.

All three developed gelatin-based active biodegradable hydrogel films showed broad of O–H/N–H stretching bands at 3302–3303 cm^{-1}, indicating extensive hydrogen bonding within the polymer network [24,25]. The broadest peak was observed in S1 film, suggesting a higher contribution from polysaccharide-based components [26], whereas S2 and S3 films exhibited comparatively sharper bands consistent with stronger protein-mediated interactions at higher gelatin concentrations [27]. Peaks in the 2924–2930 cm^{-1} region and associated CH_2 symmetric vibrations (~2854–2884 cm^{-1}) were present in all formulations and corresponded to

aliphatic C–H stretching of fatty acids and phospholipid chains from neem oil and lecithin. These peaks were more intense in S2 and S3 films, indicating more efficient lipid incorporation within the denser gelatin matrices [28].

The ester carbonyl peak near 1742–1743 cm^{-1} confirmed the presence of lipid-derived ester linkages in all films. Film S3 showed the most defined ester band, suggesting enhanced stability of the emulsified oil phase at higher gelatin content [29]. Protein-associated amide I (1642–1635 cm^{-1}) and amide II (1551–1550 cm^{-1}) bands were evident in all samples, with increasing intensity from S1 to S3 films, reflecting the progressive increase in gelatin concentration and protein network formation. These results confirm that gelatin contributed significantly to the structural organization of the hydrogel matrix [27,30].

The region between 1407–1038 cm^{-1} showed characteristic vibrations corresponding to COO^- stretching, O–H bending, C–N stretching, and C–O–C linkages originating from various polysaccharides and stabilizing agents [31]. S1 film demonstrated stronger polysaccharide-derived signals such as pectin, mannitol, and pullulan, consistent with a more hydrated and flexible structure [31,32]. S2 film exhibited balanced polysaccharide-protein features including guar gum, agarose, and casein, while S3 film showed characteristic interactions from alginate, chitosan, cellulose acetate, and xanthan gum, indicating the presence of a more compact and reinforced biopolymer network [33].

FTIR analysis revealed distinct formulation dependent variations among the gelatin-based hydrogel films. S1 film showed dominant polysaccharide driven hydrogen bonding which supports its higher flexibility, while S2 film displayed a balanced contribution of proteins, polysaccharides, and lipids indicating an intermediate structural organization. In comparison, S3 film demonstrated the most pronounced protein dominant structure with enhanced lipid stabilization, reflecting the formation of a denser and more compact gelatin-based hydrogel matrix. These structural differences directly correlated with the mechanical and barrier behaviors of the films.

3.2 Mechanical properties of developed gelatin-based hydrogel films

Mechanical properties of the gelatin-based hydrogel films showed a clear dependence on gelatin concentration and results are tabulated in **Table 3**. S1 film demonstrated the highest tensile strength at 0.203 ± 0.012 MPa and the highest elongation at 248.9 ± 4.33 %, which supports the FTIR observation that this film contained a polysaccharide rich and highly hydrated matrix capable of substantial deformation [34,35]. S2 film exhibited intermediate

values, with a tensile strength of 0.148 ± 0.010 MPa and elongation of 205.27 ± 3.18 %, which reflects its balanced polymer composition that allows both structural resistance and reasonable flexibility. S3 film displayed the lowest tensile strength at 0.091 ± 0.013 MPa and the lowest elongation at 189.07 ± 3.68 %. This pattern is consistent with the compact, protein-dominant structure determined by FTIR, because densely packed protein chains lower molecular mobility and limit deformation when subjected to stress [35].

The gradual reduction in mechanical properties with increasing gelatin concentration suggests that lower protein levels facilitated enhanced chain mobility and more efficient stress distribution, resulting in greater elasticity [35,36]. These findings are consistent with previous studies on gelatin and protein based hydrogels where higher protein concentrations create rigid networks that limit chain relaxation and tend to fracture more readily [37-40].

Lower concentrations, as observed in S1 film, often promote softer and more elastic matrices, although such flexibility may come at the expense of structural stability under mechanical load [34,41]. The performance of the S2 film positions it as the most mechanically balanced formulation because it combines adequate strength with sufficient extensibility, a combination that is desirable for films intended for active food packaging where both stability and compliance are required.

3.3 Barrier properties of developed gelatin-based hydrogel films

The results for barrier properties of all gelatin-based hydrogel film formulations, including WVTR and OTR, are tabulated in **Table 3**. As gelatin concentration increased, WVTR decreased, and these results are reported in **Table 3**.

Film S1 recorded the highest WVTR (54.10 ± 1.51 $g \cdot m^{-2} \cdot day^{-1}$), followed by film S2 (48.33 ± 1.31 $g \cdot m^{-2} \cdot day^{-1}$), while film S3 displayed the lowest WVTR (46.06 ± 1.16 $g \cdot m^{-2} \cdot day^{-1}$). This reduction with increasing polymer concentration suggests that denser hydrogel matrices in higher-gelatin films provided improved resistance to moisture permeation. This trend aligns with previous reports where increased biopolymer content reduces free volume and restricts water vapour diffusion [42-44].

A similar trend was observed for OTR analysis. The highest OTR was measured for film S1 (210 ± 4.08 $cm^3 \cdot m^{-2} \cdot day^{-1} \cdot atm^{-1}$), which decreased to 191.67 ± 6.24 $cm^3 \cdot m^{-2} \cdot day^{-1} \cdot atm^{-1}$ for film S2 and further to 181.67 ± 6.24 $cm^3 \cdot m^{-2} \cdot day^{-1} \cdot atm^{-1}$ for film S3. The reduced OTR values with increasing gelatin concentration suggest the formation of a more compact and uniform matrix, limiting oxygen diffusion [43]. Comparable findings in gelatin-

based and hydrogel-based packaging films show that increased protein concentration enhances oxygen barrier performance due to stronger polymer chain interactions and reduced microvoids [42,45].

The combined WVTR and OTR results suggest that stronger protein interactions and greater molecular packing in S3 film generate fewer diffusion pathways for moisture and gases. In contrast, the higher permeability of S1 film is attributed to its more hydrated and open network, characteristic of polysaccharide-rich matrices. Positioned between these extremes, S2 film demonstrates intermediate barrier performance, indicating a sufficiently compact structure that offers meaningful protection without excessive rigidity.

Considering the functional, mechanical, and barrier results collectively, each formulation demonstrated distinct functional strengths. Film S1 showed high flexibility but insufficient barrier protection, while S3 film offered strong moisture and oxygen resistance but limited mechanical resilience. In contrast, S2 film presented the most balanced performance, combining adequate tensile, desirable elongation, and moderate barrier properties suitable for protecting perishable foods. Therefore, S2 film was selected as the optimized gelatin-based hydrogel film for thermal, morphological, microbial, and biodegradability evaluations to assess its potential for biodegradable active food packaging applications.

3.4 Thermal properties of selected gelatin-based hydrogel film

DSC analysis revealed distinct thermal transitions reflecting the structural organization and thermal stability of the developed gelatin-based hydrogel film, and the results are presented in **Table 4**. At the lower temperature range, the DSC thermogram exhibited two distinct Tg temperatures which confirm the presence of more than one amorphous domain within the hydrogel network. The Tg_1 occurred at 39.09 °C with the onset (To_1) and endset (Tc_1) temperatures recorded at 35.02 °C and 43.26 °C, respectively. The Tg_2 appeared at 51.92 °C. The corresponding changes in specific heat capacity (ΔCp) were 0.207 J g^{-1} $°C^{-1}$ for Tg_1 and 0.172 J g^{-1} $°C^{-1}$ for Tg_2. The occurrence of two glass transition points indicates partial phase separation between the hydrophilic and hydrophobic regions of the film [46].

The lower glass transition corresponds to the gelatin and glycerol-rich region, which shows greater molecular flexibility due to the plasticizing effect of glycerol. The higher transition temperature is related to the lecithin and neem oil region where restricted molecular mobility results in a more rigid phase [46]. This dual glass transition pattern is common in composite biopolymer systems containing both hydrophilic and hydrophobic components [47].

The partial incompatibility between these domains produces a heterogeneous network structure. Similar behavior has been reported in gelatin film blended with plasticizers, where microphase separation leads to multiple transition zones [48].

A strong endothermic peak was observed in the second thermogram, which represents the melting or structural disintegration of the organized polymeric regions. The melting transition began at 185.60 °C (To_2), reached a maximum peak at 188.70 °C (Tm), and completed at 196.92 °C (Tc_2). The ΔH change associated with this event was 156.4837 $J \cdot g^{-1}$. The sharp and narrow nature of the endothermic peak indicates the existence of ordered crystalline domains that require significant energy to disrupt. These ordered regions are most likely formed through intermolecular hydrogen bonding between gelatin chains and lecithin molecules, along with the contribution of triple-helical structures in the gelatin matrix [21,49].

The high value of enthalpy reflects strong cohesive interactions within the film and confirms the presence of a semi-crystalline structure. The melting temperature near 189 °C demonstrates that the gelatin-based hydrogel film possesses good thermal stability and can tolerate moderate processing and storage temperatures without losing its structural integrity. The combined presence of glycerol, soy lecithin, and neem oil effectively modulates the molecular arrangement of the hydrogel, resulting in an optimized balance between elasticity and thermal endurance. These characteristics make the developed gelatin-based hydrogel film suitable for biodegradable and functional packaging applications that demand mechanical flexibility and resistance to thermal degradation.

3.5 Morphological analysis of selected gelatin-based hydrogel film

The surface morphology of the developed gelatin-based hydrogel film was examined using FE-SEM at both low (100X) and high (1200X) magnifications to evaluate the uniformity, phase dispersion, and internal microstructure of the film matrix. The micrograph obtained at 100X magnification (**Fig. 2a**) revealed a smooth, compact, and continuous surface with a few shallow depressions and minor voids. This observation suggests that the film formation process produced a homogeneous gelatin-based network without cracks or fractures [15,50]. The dense matrix structure indicates strong polymer chain entanglement and effective cross-linking between the biopolymer and plasticizer components, ensuring flexibility and mechanical stability of the film [51].

At a higher magnification of 1200X (**Fig. 2b**), the film displayed a dense polymeric network with uniformly distributed micro-sized pores and spherical cavities. The pore

diameters ranged from approximately 3.95 to 8.98 µm, which can be attributed to entrapped air bubbles or phase separation between the hydrophilic gelatin matrix and the dispersed hydrophobic domains, such as neem oil stabilized by soy lecithin. These microcavities indicate successful emulsification and uniform dispersion of the oil phase within the continuous gelatin network [50]. The absence of large aggregates or fractured edges further confirms that the incorporation of bioactive ingredients maintained the films structural integrity while enhancing compactness and cohesion [52].

Such microstructural characteristics are in good agreement with previously reported emulsion-based hydrogel and biopolymer films [53,54]. Pure gelatin films generally exhibit smoother and more featureless surfaces due to the presence of a single continuous phase [55,56]. However, the incorporation of hydrophobic bioactive compounds or essential oils often produces a slightly rougher texture with discrete voids and embedded droplets. This pattern has been reported in gelatin films containing clove, oregano, and citrus essential oils [57,58]. The presence of fine and uniformly distributed microvoids within the 3-10 µm range is consistent with the findings of Li *et al*., [59,60] who linked such porosity to improved swelling behavior, diffusivity, and retention of active compounds in gelatin-polysaccharide composite hydrogels.

The developed gelatin-based hydrogel film exhibited a moderately porous yet continuous microstructure, which played a significant role in defining its functional performance. The compact and well-connected polymeric network contributed to improved mechanical strength and effective barrier properties [61], while the presence of fine, uniformly distributed pores enhanced water uptake and diffusion behavior [62]. These microvoids likely facilitated the controlled and sustained release of neem oil and other bioactive constituents embedded within the gelatin-lecithin matrix. Such structural characteristics are advantageous for maintaining prolonged antimicrobial and antioxidant activity during application [63,64]. Comparable morphological and functional relationships has been reported by Bhardwaj *et al*., [65] on gelatin based hydrogel systems, where controlled porosity was found to enhance swelling, permeability, and active compound release. Therefore, the observed morphology in the present study confirms that the developed gelatin-based hydrogel film possesses an optimized structure suitable for smart and active food packaging applications.

3.6 Microbial stability of selected gelatin-based hydrogel film

The microbiological stability of the selected S2 gelatin-based hydrogel film was evaluated through TPC analysis during refrigerated storage to determine their ability to prevent microbial contamination over time. The TPC values recorded for the selected S2 gelatin-based hydrogel film remained below detectable limits (<10 CFU/mL) on Day 1, Day 15, and Day 30 of storage, confirming the absence of microbial growth throughout the study period. These findings clearly indicate that the hydrogel film maintained excellent microbial stability and provided a contamination-free surface under refrigerated conditions (4 ± 1 °C).

The consistently undetectable TPC values demonstrate the active performance of the formulated S2 gelatin-based hydrogel film. This activity can be attributed to the presence of neem oil, which contains potent antimicrobial constituents such as azadirachtin, nimbin, and salannin that effectively inhibit bacterial proliferation [66]. The emulsifying role of soy lecithin helped achieve uniform dispersion of neem oil droplets within the gelatin matrix, enabling gradual and sustained release of the active compounds during storage [67]. Additionally, the dense and continuous surface morphology observed in the FE-SEM analysis may have acted as a physical barrier, reducing microbial attachment and penetration on the film surface.

The selected S2 gelatin-based active biodegradable hydrogel film incorporated with essential oils maintained microbial counts below detectable limits (TPC <10 CFU/mL) after 30 days of cold storage due to the sustained release of natural antimicrobial compounds [68-71]. The present study showed similar results, where the developed gelatin-based hydrogel film effectively inhibited microbial proliferation throughout the 30-day refrigerated storage period. This strong and long-lasting antimicrobial performance can be attributed to the synergistic action of the natural bioactive components and the stable polymeric matrix, which together provided an effective barrier against microbial contamination. These results confirm the potential of the developed gelatin-based hydrogel film as an active and biodegradable packaging material capable of extending the shelf life and maintaining the microbial safety of perishable food products.

3.7 Biodegradability of selected gelatin-based hydrogel film

The results showed a clear trend of progressive decomposition of the gelatin-based hydrogel film with increasing burial time. At the beginning of the test, the gelatin-based hydrogel film retained its structural integrity and smooth appearance. After 3 days of burial, the surface became slightly softer with minor loss of transparency, indicating the initiation of microbial activity and water absorption by the biopolymer matrix. By the 6th day, small cracks and color

fading were evident on the surface, suggesting the partial breakdown of the gelatin network due to microbial colonization [62]. On the 9th day, the film exhibited visible fragmentation and an average weight loss of approximately 56.3 ± 2.1 %, confirming enzymatic degradation and hydrolysis of the polymer chains [72]. After 12th day, the film showed extensive disintegration with only small pieces remaining, corresponding to about 83.7 ± 1.8 % degradation. Complete degradation was observed on the 15th day with a total weight loss of 96.4 ± 1.2 %, leaving only fine traces of organic residue in the soil.

The rapid and complete decomposition within 15 days demonstrates the high biodegradation potential of the developed gelatin-based hydrogel film. This behavior can be attributed to the natural biodegradability of the film components including gelatin, glycerol, soy lecithin, and neem oil. The hydrophilic and moderately porous structure of the film, as confirmed by FE-SEM analysis, enhanced soil moisture infiltration and microbial accessibility, promoting faster enzymatic hydrolysis. Microorganisms present in the soil produced proteases and lipases that efficiently degraded the peptide and ester bonds within the biopolymer matrix [73]. Although neem oil and lecithin introduced mild hydrophobicity, their concentrations were insufficient to hinder microbial attack, allowing continuous degradation throughout the test period.

The biodegradation rate observed in this study corresponds well with earlier reports on gelatin-based biodegradable films. Mottalib *et al*., [74] reported approximately 80 % degradation of gelatin-starch composites within 15 days, while Li *et al*., [60] observed near-complete breakdown of gelatin film incorporated with essential oils within 12 to 16 days. Similarly, Said *et al*., [75] found that gelatinchitosan films degraded completely within 14 days under comparable soil conditions. The results of the present study, showing complete degradation of the gelatin-based hydrogel film within 15 days, are consistent with these reports and confirm its rapid biodegradability and environmental compatibility. The film exhibited controlled degradation behavior that maintained structural stability during use and ensured total disintegration after disposal. These characteristics highlight its suitability as a sustainable material for active food packaging, offering both functional performance and ecological safety.

3.8. Visual shelf life assessment of cherry tomatoes under refrigerated storage

The practical performance of the selected S2 gelatin-based hydrogel film was assessed by tracking the visual quality of cherry tomatoes kept in refrigerated storage at 4 ± 1 °C. The control tomatoes were stored in transparent PET clamshell containers, whereas the treated

tomatoes were packaged in PET clamshell containers using the S2 gelatin-based hydrogel film. Visual observations were undertaken at every three days intervals on the storage of 0, 3, 6, 9, 12, and 15 days, as depicted in **Fig. 3**.

On the 0th day, both treatments showed a fresh, intact external appearance with no observable surface shrinkage. Similar appearances persisted on 3rd and 6th days, and neither treatment exhibited distinct surface shrinkage up to 9th day. By 12th day, visible surface shrinkage became apparent in the control tomatoes, signaling the start of noticeable visual deterioration, while the S2 gelatin-based hydrogel film packaged tomatoes maintained a comparatively better appearance. Surface shrinkage was also evident in the S2 hydrogel film packaged tomatoes by 15th day.

Based on the first appearance of visible surface shrinkage, the apparent visual shelf life was estimated at about 12 days for the control and 15 days for the S2 gelatin-based hydrogel film packaged tomatoes, corresponding to a 3 days delay in the onset of visible surface deterioration. This delayed shrinkage may relate to the barrier properties of the S2 gelatin-based hydrogel film and its ability to moderate moisture transfer; however, moisture loss was not measured directly in this study.

The observed pattern agrees with prior findings on gelatin-based packaging systems. Sooch and Mann (2021) [76], reported prolonged tomato shelf life using a Ti-doped CuO-reinforced gelatin active packaging film, and other gelatin-based composite films incorporating antimicrobial, antioxidant, neem essential-oil, or cellulose nanofiber components have been reported to reduce weight loss and slow quality deterioration in tomatoes. Meaningful comparison may be constrained owing to the fact that reported studies varied in film matrix formulation, active components, storage environment, packaging configuration, and criteria used for shelf life assessment.

Therefore, the 3-day prolongation observed in the present study should be interpreted as an apparent extension of visual shelf life based primarily on the onset of visible surface shrinkage, not as a comprehensive assessment of physico-chemical, microbiological, or sensory quality. Overall, the S2 gelatin-based hydrogel film exhibited potential for delaying visible surface shrinkage and retaining the visual appearance of cherry tomatoes throughout refrigerated storage.

4. Conclusion

The developed gelatin-based hydrogel films demonstrated desirable functional, mechanical, barrier, thermal, morphological, microbial, and biodegradation properties, indicating their potential for sustainable active food-packaging applications. Based on the combined mechanical and barrier performance, S2 was identified as the most suitable formulation, with a tensile strength of 0.148 ± 0.010 MPa, elongation at break of 205.27 ± 3.18%, WVTR of 48.33 ± 1.31 $g \cdot m^{-2} \cdot day^{-1}$, and OTR of 191.67 ± 6.24 $cm^3 \cdot m^{-2} \cdot day^{-1} \cdot atm^{-1}$. FTIR analysis indicated interactions among gelatin, soy lecithin, and neem oil, while DSC showed Tg_1 of 39.09 °C, Tg_2 of 51.92 °C, and Tm of 188.70 °C. FE-SEM revealed a compact surface with micropores ranging from 3.95 to 8.98 µm. The selected film maintained a total plate count below the detection limit (<10 CFU/mL) during the 30-day evaluation and exhibited 96.4 ± 1.2% biodegradation within 15 days under aerobic soil conditions. In the cherry tomato application study, the selected S2 hydrogel film delayed the onset of visible surface shrinkage by approximately 3 days, with shrinkage observed on day 12 in the control and day 15 in the hydrogel-film packaged tomatoes. Based on this visual criterion, the film demonstrated potential to maintain the visual quality and extend the apparent shelf life of cherry tomatoes under refrigerated conditions while providing active biodegradable packaging functionality.

CRediT authorship contribution statement

ND: Investigation, Writing - Original draft preparation, Methodology; **RG:** Investigation, Writing - Original draft, Methodology; **HP:** Validation, Methodology, Software; **MSS:** Reviewing and Editing; **PBP:** Validation, Supervision, Reviewing and Editing; **PSG:** Investigation, Conceptualization, Visualization; Validation, Software, Supervision, Reviewing and Editing.

Funding: Open access funding was provided by D.Y. Patil (Deemed to be University), Navi Mumbai.

Data availability: The datasets produced and/or analyzed in this study can be obtained from the corresponding author upon reasonable request.

Declaration:

Ethics and Consent to Participate declarations: Not applicable. No human participants or animals were involved in this study. The cherry tomatoes were commercially purchased from APMC Market, Vashi, Navi Mumbai, Maharashtra, India. The procurement and use of the plant

material complied with applicable local and national guidelines with no need for further affirmation.

Clinical trial number: Not applicable.

Consent to Publish declaration: Not applicable. No identifying information of individuals is included in this study.

Competing interest: The authors declare that they have no competing interests.

Acknowledgements: The authors acknowledge School of Biotechnology & Bioinformatics, D Y Patil (Deemed to be University), Navi Mumbai, Maharashtra 400614, India, for providing institutional support.

References

1. Cheng J, Gao R, Zhu Y, Lin Q. Applications of biodegradable materials in food packaging: a review. Alex Eng J. 2024;91:70-83. doi: 10.1016/j.aej.2024.01.080 .
2. Bócoli PFJ, Gomes VES, Maia AAD, Marangoni Júnior L. Perspectives on eco-friendly food packaging: challenges, solutions, and trends. Foods. 2025;14(17):3062. doi: 10.3390/foods14173062 .
3. Rudra SG, Basu S, Chanda A. Editorial: food storage, spoilage and shelf life: recent developments and insights. Front Sustain Food Syst. 2022;6:953983. doi: 10.3389/fsufs.2022.953983 .
4. Sun X, Wang J, Dong M, Zhang H, Li L, Wang L. Food spoilage, bioactive food fresh-keeping films and functional edible coatings: research status, existing problems and development trend. Trends Food Sci Technol. 2022;119:122-132. doi: 10.1016/j.tifs.2021.12.004 .
5. Bhat ZF, Bhat HF, Mohan MS, Aadil RM, Hassoun A, Aït-Kaddour A. Edible packaging systems for improved microbial quality of animal-derived foods and the role of emerging technologies. Crit Rev Food Sci Nutr. 2024;64(33):12137-12165. doi: 10.1080/10408398.2023.2248494 .
6. Wazir H, Chay SY, Zarei M, Hussin FS, Mustapha NA, Wan Ibadullah WZ, et al. Effects of storage time and temperature on lipid oxidation and protein co-oxidation of

low-moisture shredded meat products. Antioxidants (Basel). 2019;8(10):486. doi: 10.3390/antiox8100486 .

7. Dragoev SG. Lipid peroxidation in muscle foods: impact on quality, safety and human health. Foods. 2024;13(5):797. doi: 10.3390/foods13050797 .

8. Gómez-Estaca J, López-de-Dicastillo C, Hernández-Muñoz P, Catalá R, Gavara R. Advances in antioxidant active food packaging. Trends Food Sci Technol. 2014;35(1):42-51. doi: 10.1016/j.tifs.2013.10.008 .

9. Ye Z, Sun L, Xiang Q, Hao Y, Liu H, He Q, et al. Advancements of biomacromolecular hydrogel applications in food nutrition and health. J Agric Food Chem. 2024;72(43):23689-23708. doi: 10.1021/acs.jafc.4c05903 .

10. Gururani P, Bhatnagar P, Dogra P, Joshi HC, Chauhan PK, Vlaskin MS, et al. Bio-based food packaging materials: a sustainable and holistic approach for cleaner environment—a review. Curr Res Green Sustain Chem. 2023;7:100384. doi: 10.1016/j.crgsc.2023.100384 .

11. Stoica M, Bichescu CI, Crețu CM, Dragomir M, Ivan AS, Podaru GM, et al. Review of bio-based biodegradable polymers: smart solutions for sustainable food packaging. Foods. 2024;13(19):3027. doi: 10.3390/foods13193027

12. Dey B, Prabhakar MR, Jayaraman S, Gujjala LKS, Venugopal AP, Balasubramanian P. Biopolymer-based solutions for enhanced safety and quality assurance: a review. Food Res Int. 2024;191:114723. doi: 10.1016/j.foodres.2024.114723.

13. Schaschke C, Audic JL. Editorial: biodegradable materials. Int J Mol Sci. 2014;15(11):21468-21475. doi: 10.3390/ijms151121468.

14. Zhao X, Cornish K, Vodovotz Y. Narrowing the gap for bioplastic use in food packaging: an update. Environ Sci Technol. 2020;54(8):4712-4732. doi: 10.1021/acs.est.9b03755.

15. Benkhira I, Zermane F, Cheknane B, Trache D, Brosse N, Paolone A, et al. Preparation and characterization of amidated pectin-gelatin-oxidized tannic acid hydrogel films supplemented with in-situ reduced silver nanoparticles for wound-dressing applications. Int J Biol Macromol. 2024;277(Pt 1):134158. doi: 10.1016/j.ijbiomac.2024.134158.

16. Borbolla-Jiménez FV, Peña-Corona SI, Farah SJ, Jiménez-Valdés MT, Pineda-Pérez E, Romero-Montero A, et al. Films for wound healing fabricated using a solvent casting technique. Pharmaceutics. 2023;15(7):1914. doi: 10.3390/pharmaceutics15071914.
17. Tanwar M, Rani A, Gautam N, Talegaonkar S, Gupta RK. Essential oils loaded carboxymethylated Cassia fistula gum-based novel hydrogel films for wound healing. Int J Biol Macromol. 2024;278(3):134682. doi: 10.1016/j.ijbiomac.2024.134682.
18. Kuddushi M, Deng X, Nayak J, Zhu S, Xu BB, Zhang X. A transparent, tough and self-healable biopolymeric composites hydrogel for open wound management. ACS Appl Bio Mater. 2023;6(9):3810-3822. doi: 10.1021/acsabm.3c00455.
19. Salavati Hamedani M, Rezaeigolestani M, Mohsenzadeh M. Optimization of antibacterial, physical and mechanical properties of novel chitosan/olibanum gum film for food packaging application. Polymers (Basel). 2022;14(19):3960. doi: 10.3390/polym14193960.
20. Zeng J, Ma Y, Li P, Zhang X, Gao W, Wang B, et al. Development of high-barrier composite films for sustainable reduction of non-biodegradable materials in food packaging application. Carbohydr Polym. 2024;330:121824. doi: 10.1016/j.carbpol.2024.121824.
21. Wang F, Wen Y, Bai T. Thermal behavior of polyvinyl alcohol–gellan gum–Al^{3+} composite hydrogels with improved network structure and mechanical property. J Therm Anal Calorim. 2017;127(3):2447-2457. doi: 10.1007/s10973-016-5757-3.
22. Alzahrani A. Fluorescent carbon dots in situ polymerized biodegradable semi-interpenetrating tough hydrogel films with antioxidant and antibacterial activity for applications in food industry. Food Chem. 2024;447:138905. doi: 10.1016/j.foodchem.2024.138905.
23. Harrazi N, Özbek HN, Yanık DK, Zaghbib I, Göğüş F. Development and characterization of gelatin-based biodegradable films incorporated with pistachio shell hemicellulose. J Food Sci Technol. 2024;61(10):1919-1929. doi: 10.1007/s13197-024-05968-4.
24. Duan JJ, Zhang LN. Robust and smart hydrogels based on natural polymers. Chin J Polym Sci. 2017;35(10):1165-1180. doi: 10.1007/s10118-017-1983-9.
25. Wang P, Liao Q, Zhang H. Polysaccharide-based double-network hydrogels: polysaccharide effect, strengthening mechanisms, and applications. Biomacromolecules. 2023;24(12):5479-5510. doi: 10.1021/acs.biomac.3c00765.

26. Sanjanwala D, Londhe V, Trivedi R, Bonde S, Sawarkar S, Kale V, et al. Polysaccharide-based hydrogels for medical devices, implants and tissue engineering: a review. Int J Biol Macromol. 2024;256(Pt 2):128488. doi: 10.1016/j.ijbiomac.2023.128488.
27. Kazemi-Taskooh Z, Varidi M. Interaction-induced characterization of animal-based protein-polysaccharide composite hydrogels: a review. Food Rev Int. 2024;40(10):3572-3604. doi: 10.1080/87559129.2024.2366857.
28. Kaur H, Gogoi B, Sharma I, Das DK, Azad MA, Das Pramanik D, et al. Hydrogels as a potential biomaterial for multimodal therapeutic applications. Mol Pharm. 2024;21(10):4827-4848. doi: 10.1021/acs.molpharmaceut.4c00595.
29. Qi X, Wei W, Shen J, Dong W. Salecan polysaccharide-based hydrogels and their applications: a review. J Mater Chem B. 2019;7(16):2577-2587. doi: 10.1039/C8TB03312A.
30. Rather RA, Bhat MA, Shalla AH. An insight into synthetic and physiological aspects of superabsorbent hydrogels based on carbohydrate type polymers for various applications: a review. Carbohydr Polym Technol Appl. 2022;3:100202. doi: 10.1016/j.carpta.2022.100202.
31. Gieroba B, Kalisz G, Krysa M, Khalavka M, Przekora A. Application of vibrational spectroscopic techniques in the study of the natural polysaccharides and their cross-linking process. Int J Mol Sci. 2023;24(3):2630. doi: 10.3390/ijms24032630.
32. Fanova A, Sotiropoulos K, Radulescu A, Papagiannopoulos A. Advances in small angle neutron scattering on polysaccharide materials. Polymers (Basel). 2024;16(4):490. doi: 10.3390/polym16040490.
33. Derkach SR, Voron'ko NG, Kuchina YA. Intermolecular interactions in the formation of polysaccharide-gelatin complexes: a spectroscopic study. Polymers (Basel). 2022;14(14):2777. doi: 10.3390/polym14142777.
34. He Q, Huang Y, Wang S. Hofmeister effect-assisted one-step fabrication of ductile and strong gelatin hydrogels. Adv Funct Mater. 2018;28(5):1705069. doi: 10.1002/adfm.201705069.
35. Yousefi-Mashouf H, Bailly L, Orgéas L, Henrich Bernardoni N. Mechanics of gelatin-based hydrogels during finite strain tension, compression and shear. Front Bioeng Biotechnol. 2023;10:1094197. doi: 10.3389/fbioe.2022.1094197.
36. Chen S, Ravi-Chandar K. Nonlinear poroviscoelastic behavior of gelatin-based hydrogel. J Mech Phys Solids. 2022;158:104650. doi: 10.1016/j.jmps.2021.104650.

37. Melzak KA, Mateescu A, Toca-Herrera JL, Jonas U. Simultaneous measurement of mechanical and surface properties in thermoresponsive, anchored hydrogel films. Langmuir. 2012;28(35):12871-12878. doi: 10.1021/la3019666.
38. Kirchmajer DM, in het Panhuis M. Robust biopolymer based ionic-covalent entanglement hydrogels with reversible mechanical behaviour. J Mater Chem B. 2014;2(29):4694-4702. doi: 10.1039/c4tb00258j.
39. Zhu FB, Yu HC, Lei WX, Ren KF, Qian J, Wu ZL, et al. Tough polyion complex hydrogel films of natural polysaccharides. Chin J Polym Sci. 2017;35(10):1276-1285. doi: 10.1007/s10118-017-1977-7.
40. Sun X, Liang Y, Ye L, Liang H. An extremely tough and ionic conductive natural-polymer-based double network hydrogel. J Mater Chem B. 2021;9(37):7751-7759. doi: 10.1039/d1tb01458g.
41. Wang M, Sun S, Dong G, Long F, Butcher JT. Soft, strong, tough, and durable protein-based fiber hydrogels. Proc Natl Acad Sci U S A. 2023;120(8):e2213030120. doi: 10.1073/pnas.2213030120.
42. Benbettaïeb N, Kurek M, Bornaz S, Debeaufort F. Barrier, structural and mechanical properties of bovine gelatin-chitosan blend films related to biopolymer interactions. J Sci Food Agric. 2014;94(12):2409-2419. doi: 10.1002/jsfa.6570.
43. Tyuftin AA, Pecorini F, Zanardi E, Kerry JP. Parameters affecting the water vapour permeability of gelatin films as evaluated by the infrared detecting method ASTM F1249. Sustainability. 2022;14(15):9018. doi: 10.3390/su14159018.
44. Fu ZQ, Zheng ZX, Li Y, Guo SX, Gao DM, Li FF. Potato flour-based film: effect of gelatine on the rheological, thermal, mechanical and barrier properties. Int J Food Sci Technol. 2024;59(9):5877-5885. doi: 10.1111/ijfs.17352.
45. Ahmed S, Ikram S. Chitosan and gelatin based biodegradable packaging films with UV-light protection. J Photochem Photobiol B. 2016;163:115-124. doi: 10.1016/j.jphotobiol.2016.08.023.
46. Salmerón Sánchez M, Gallego Ferrer G, Monleón Pradas M, Gómez Ribelles JL. Influence of the hydrophobic phase on the thermal transitions of water sorbed in a polymer hydrogel based on interpenetration of a hydrophilic and a hydrophobic network. Macromolecules. 2003;36(3):860-866. doi: 10.1021/ma021069p.
47. Cerqueira Barros S, Alves da Silva A, Costa CM, Lanceros-Méndez S, Barbosa Costa D, Tamano Maciavello M, et al. Thermal-mechanical behaviour of chitosan-cellulose

derivative thermoreversible hydrogel films. Cellulose. 2015;22(3):1911-1929. doi: 10.1007/s10570-015-0603-5.

48. Duan Q, Chen Y, Yu L, Xie F. Chitosan-gelatin films: plasticizers/nanofillers affect chain interactions and material properties in different ways. Polymers (Basel). 2022;14(18):3797. doi: 10.3390/polym14183797.
49. Tsioptsias C, Fardis D, Ntampou X, Tsivintzelis I, Panayiotou C. Thermal behavior of poly(vinyl alcohol) in the form of physically crosslinked film. Polymers (Basel). 2023;15(8):1843. doi: 10.3390/polym15081843.
50. Khairan K, Hasan M, Idroes R, Diah M. Fabrication and evaluation of polyvinyl alcohol/corn starch/patchouli oil hydrogel films loaded with silver nanoparticles biosynthesized in Pogostemon cablin Benth leaves' extract. Molecules. 2023;28(5):2020. doi: 10.3390/molecules28052020.
51. Wu Y, Wang X, Zhou Y, Wu S, Peng L, Tian J, et al. Gelatin/cinnamon essential oil Pickering emulsion crosslinking composite films with enhanced mechanical and antibacterial performance. J Food Eng. 2024;371:111992. doi: 10.1016/j.jfoodeng.2024.111992.
52. Hasan N, Cao J, Lee J, Kim HW, Yoo JW. Development of clindamycin-loaded alginate/pectin/hyaluronic acid composite hydrogel film for the treatment of MRSA-infected wounds. J Pharm Investig. 2021;51(5):597-610. doi: 10.1007/s40005-021-00541-z.
53. Esquirol AL, Sarazin P, Virgilio N. Tunable porous hydrogels from cocontinuous polymer blends. Macromolecules. 2014;47(9):3068-3075. doi: 10.1021/ma402603b.
54. Li D, Li EJ, Li L, Li B, Jia S, Xie Y, et al. Effect of TEMPO-oxidized bacterial cellulose nanofibers stabilized Pickering emulsion of cinnamon essential oil on structure and properties of gelatin composite films. Int J Biol Macromol. 2024;264(Pt 1):130344. doi: 10.1016/j.ijbiomac.2024.130344.
55. Wisotzki EI, Hennes M, Schuldt C, Engert F, Knolle W, Decker U, et al. Tailoring the material properties of gelatin hydrogels by high energy electron irradiation. J Mater Chem B. 2014;2(27):4297-4309. doi: 10.1039/c4tb00429a.
56. Kaberova Z, Karpushkin E, Nevoralová M, Vetrík M, Šlouf M, Dušková-Smrčková M. Microscopic structure of swollen hydrogels by scanning electron and light microscopies: artifacts and reality. Polymers (Basel). 2020;12(3):578. doi: 10.3390/polym12030578.

753 57. Wang S, Li L, Su D, Robin K, Brown KA. Patterning porosity in hydrogels by arresting
754 phase separation. ACS Appl Mater Interfaces. 2018;10(40):34604-34610. doi:
755 10.1021/acsami.8b11530.
756 58. Gelli R, Mugnaini G, Bolognesi T, Bonini M. Cross-linked porous gelatin
757 microparticles with tunable shape, size, and porosity. Langmuir. 2021;37(44):12781-
758 12789. doi: 10.1021/acs.langmuir.1c01508.
759 59. Li G, Zhou Q, Liu S, Qian C, Han J, Zhou T, et al. Effect of Tribute citrus essential oil
760 nanoemulsion-loaded gelatin on the gel behavior and gelation surface morphologies.
761 Food Biosci. 2023;51:102322. doi: 10.1016/j.fbio.2022.102322.
762 60. Li M, Guo L, Mu Y, Huang X, Jin L, Xu Q, et al. Gelatin films reinforced by tannin-
763 nanocellulose microgel with improved mechanical and barrier properties for
764 sustainable active food packaging. Food Hydrocoll. 2024;149:109642. doi:
765 10.1016/j.foodhyd.2023.109642.
766 61. Shan P, Wang K, Sun F, Li Y, Sun L, Li H, et al. Humidity-adjustable functional gelatin
767 hydrogel/ethyl cellulose bilayer films for active food packaging application. Food
768 Chem. 2024;439:138202. doi: 10.1016/j.foodchem.2023.138202.
769 62. Yang H, Li L, Li C, Xu Z, Tao Y, Lu J, et al. Multifunctional and antimicrobial
770 carboxymethyl cellulose-based active hydrogel film for fruits packaging and
771 preservation. Food Biosci. 2024;59:104005. doi: 10.1016/j.fbio.2024.104005.
772 63. Gong W, Yang TQ, He WY, Li YX, Hu JN. On-demand removable hydrogel film
773 derived from gallic acid-phycocyanin and polyvinyl alcohol for fruit preservation. Food
774 Chem. 2025;463(Pt 4):141404. doi: 10.1016/j.foodchem.2024.141404.
775 64. Li K, Qiao S, Yan J, Shi Z, Zhu S, Cui Z. Interconnected porous hydrogels stabilized
776 by polyphenol nanoparticles with antibacterial and antioxidant properties for skin
777 wound repair. ACS Appl Bio Mater. 2025;8(10):8829-8844. doi:
778 10.1021/acsabm.5c00970.
779 65. Bhardwaj D, Bhaskar R, Sharma AK, Garg M, Han SS, Agrawal G.
780 Gelatin/polyacrylamide-based antimicrobial and self-healing hydrogel film for wound
781 healing application. ACS Appl Bio Mater. 2024;7(2):879-891. doi:
782 10.1021/acsabm.3c00903.
783 66. Wylie MR, Merrell DS. The antimicrobial potential of the neem tree Azadirachta
784 indica. Front Pharmacol. 2022;13:891535. doi: 10.3389/fphar.2022.891535.

67. Lin L, Fang H, Li C, Dai J, Alharbi M, Cui H. Advancing gelatin/cinnamaldehyde O/W emulsions electrospinability: role of soybean lecithin in core-shell nanofiber fabrication. Food Chem. 2024;449:139305. doi: 10.1016/j.foodchem.2024.139305.
68. Kuorwel KK, Cran MJ, Sonneveld K, Miltz J, Bigger SW. Essential oils and their principal constituents as antimicrobial agents for synthetic packaging films. J Food Sci. 2011;76(9):R164-R177. doi: 10.1111/j.1750-3841.2011.02384.x.
69. Fernández-Pan I, Royo M, Maté JI. Antimicrobial activity of whey protein isolate edible films with essential oils against food spoilers and foodborne pathogens. J Food Sci. 2012;77(7):M383-M390. doi: 10.1111/j.1750-3841.2012.02752.x.
70. Sharma S, Barkauskaite S, Duffy B, Jaiswal AK, Jaiswal S. Characterization and antimicrobial activity of biodegradable active packaging enriched with clove and thyme essential oil for food packaging application. Foods. 2020;9(8):1117. doi: 10.3390/foods9081117.
71. Zhang X, Zhang B, Mao R, Huang Z, Jing K, Jin C, et al. A novel multilayer film based on sodium alginate/κ-carrageenan-gelatin incorporated with ZnO nanoparticles and oregano essential oil for active food packing. Prog Org Coat. 2024;187:108170. doi: 10.1016/j.porgcoat.2023.108170.
72. La Fuente Arias CI, González-Martínez C, Chiralt A. Biodegradation behavior of poly(3-hydroxybutyrate-co-3-hydroxyvalerate) containing phenolic compounds in seawater in laboratory testing conditions. Sci Total Environ. 2024;944:173920. doi: 10.1016/j.scitotenv.2024.173920.
73. Garcia-Garcia A, Muñana-González S, Lanceros-Mendez S, Ruiz-Rubio L, Perez Alvarez L, Vilas-Vilela JL. Biodegradable natural hydrogels for tissue engineering, controlled release, and soil remediation. Polymers (Basel). 2024;16(18):2599. doi: 10.3390/polym16182599.
74. Mottalib MA, Islam MH, Dhar MC, Akhtar K, Goni MA. Preparation and characterization of new biodegradable packaging materials based on gelatin extracted from Tenualosa ilisha fish scales with cellulose nanocrystals. ACS Omega. 2024;9(52):51175-51190. doi: 10.1021/acsomega.4c07015.
75. Said NS, Howell NK, Sarbon NM. A review on potential use of gelatin-based film as active and smart biodegradable films for food packaging application. Food Rev Int. 2023;39(2):1063-1085. doi: 10.1080/87559129.2021.1929298.

76. Sooch BS, Mann MK. Nanoreinforced biodegradable gelatin based active food packaging film for the enhancement of shelf life of tomatoes (*Solanum lycopersicum* L.). Food Control. 2021;130:108322. doi: 10.1016/j.foodcont.2021.108322.

Figure Captions

Fig. 1 Packaged cherry tomatoes (a – Control Sample; b – Treatment sample with selected gelatin-based hydrogel film) stored in transparent PET clamshell containers under refrigerated (at 4 ± 1 °C) storage.

Fig. 2 Morphological analysis of the selected S2 gelatin-based hydrogel film at 100× (a) and 1, 200× (b).

Fig. 3 Visual shelf life assessment of cherry tomatoes (a – Control Sample; b – Treatment sample packaged with selected gelatin-based hydrogel film) stored in transparent PET clamshell containers under refrigerated (at 4 ± 1 °C) storage.

Table Captions

Table 1. Composition of biodegradable gelatin-based hydrogel packaging films with different formulations

Table 2. Intermolecular interactions in gelatin-based hydrogel films with different formulations (S1, S2, and S3) using FTIR spectroscopy

Table 3. Mechanical and barrier properties of developed gelatin-based hydrogel films with different formulations

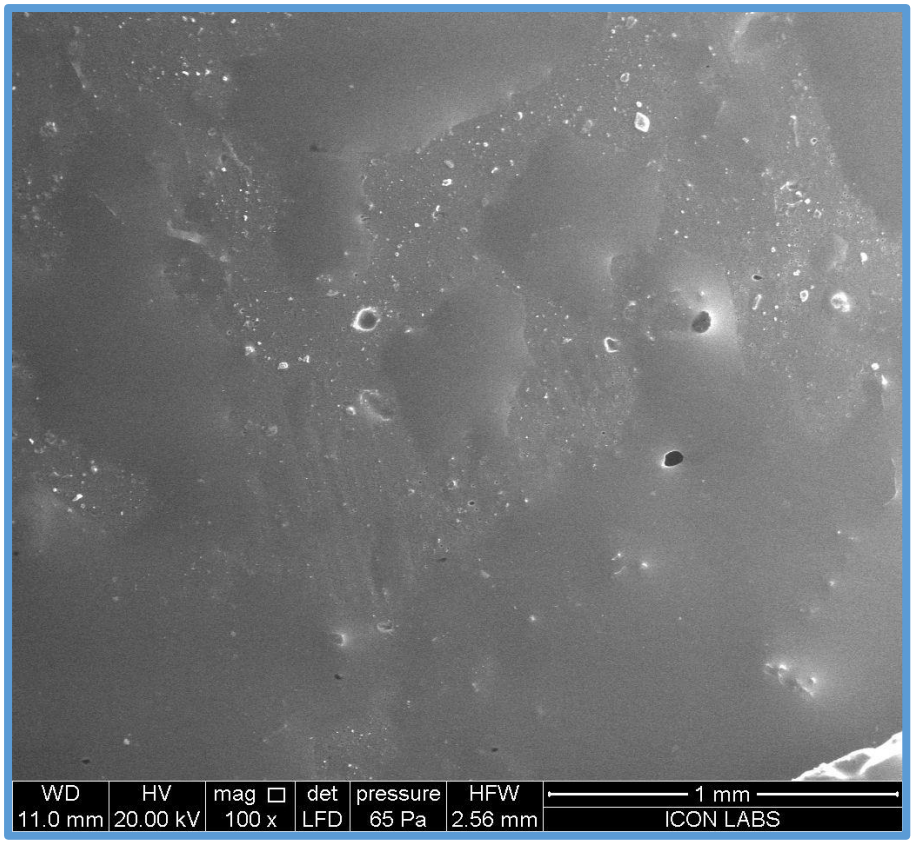
Table 4. Thermal transition characteristics of the selected S2 gelatin-based hydrogel film determined using DSC

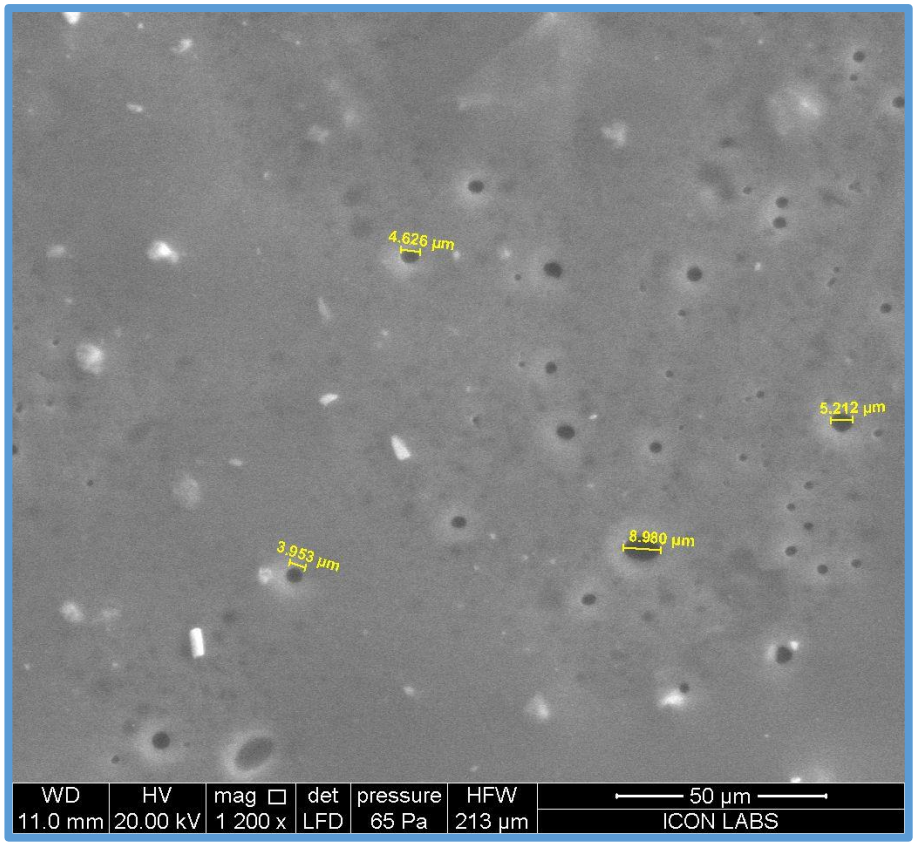
Graphical Abstract: Development of gelatin-based active biodegradable hydrogel packaging film.



(a) **(b)**

Fig. 1. Packaged cherry tomatoes (a – Control Sample; b – Treatment sample with selected gelatin-based hydrogel film) stored in transparent PET clamshell containers under refrigerated (at 4 ± 1 °C) storage.





847

848 **(a)** **(b)**

849 **Fig. 2.** Morphological analysis of the selected S2 gelatin-based hydrogel film at 100× (a) and 1, 200× (b).



(a – 0th Day) **(b – 0th Day)** **(a – 3rd Day)** **(b – 3rd Day)** **(a – 6th Day)** **(b – 6th Day)**



(a – 9th Day) **(b – 9th Day)** **(a – 12th Day)** **(b – 12th Day)** **(a – 15th Day)** **(b – 15th Day)**

Fig. 3. Visual shelf life assessment of cherry tomatoes (a – Control Sample; b – Treatment sample packaged with selected gelatin-based hydrogel film) stored in transparent PET clamshell containers under refrigerated (at 4 ± 1 °C) storage.

Table 1

Composition of biodegradable gelatin-based hydrogel packaging films with different formulations

Ingredients	**S1 (%)**	**S2 (%)**	**S3 (%)**
Soy Lecithin	2	2	2
Neem Oil	4	4	4
Gelatin	2.5	5	7.5
Glycerol	5	5	5
Distilled Water	85.5	83	80.5
Citric Acid	1	1	1
Total	**100**	**100**	**100**

Table 2

Intermolecular interactions in gelatin-based hydrogel films with different formulations (S1, S2, and S3) using FTIR spectroscopy

Sr. no.	Functional group	Molecular motion	Wavenumber (cm^{-1})			Peak variation, Δν (cm^{-1})
			S1 Film	S2 Film	S3 Film	
1	O–H / N–H	Stretching	3303.04	3302.69	3302.92	0.35
2	Aliphatic C–H	Stretching	2924.64	2929.66	2930.23	5.59
3	CH_2 / C–H	Stretching	—	2883.48	2884.26	0.78
4	CH_2	Stretching	2854.20	2855.08	2854.66	0.88
5	Ester carbonyl (C=O)	Stretching	1742.41	1743.50	1741.99	1.51
6	Amide I	C=O stretching	1635.69	1642.51	1642.89	7.20
7	Amide II	N–H bending and C–N stretching	1550.62	1551.61	1550.94	0.99
8	CH_2	Bending	1454.04	—	—	—
9	Carboxylate (COO^-)	Symmetric stretching	1406.90	1407.33	1407.39	0.49
10	C–H / O–H / C–N	Bending / deformation	1336.04	1335.72	1335.87	0.32
11	Amide III	C–N stretching and N–H bending	1238.07	1240.26	1236.24	4.02
12	C–O–C	Stretching	1203.63	—	—	—
13	C–O–C / P–O	Stretching	—	1109.95	1109.85	0.10
14	C–O	Stretching	1039.53	1038.32	1038.58	1.21

*Δν represents the difference between the highest and lowest reported wavenumbers for a given spectral band. Dashes indicate bands not reported in the supplied tables, not confirmed spectral absence.

Table 3

Mechanical and barrier properties of developed gelatin-based hydrogel films with different formulations

Film formulations	WVTR ($g \cdot m^{-2} \cdot day^{-1}$)	OTR ($cm^3 \cdot m^{-2} \cdot day^{-1} \cdot atm^{-1}$)	Tensile Strength (MPa)	Elongation (%)
S1	54.10 ± 1.51^{a}	210.00 ± 4.08^{a}	0.203 ± 0.012^{a}	248.9 ± 4.33^{a}
S2	48.33 ± 1.31^{b}	191.67 ± 6.24^{b}	0.148 ± 0.010^{b}	205.3 ± 3.18^{b}
S3	46.06 ± 1.16^{b}	181.67 ± 6.24^{b}	0.092 ± 0.013^{c}	189.07 ± 3.68^{c}

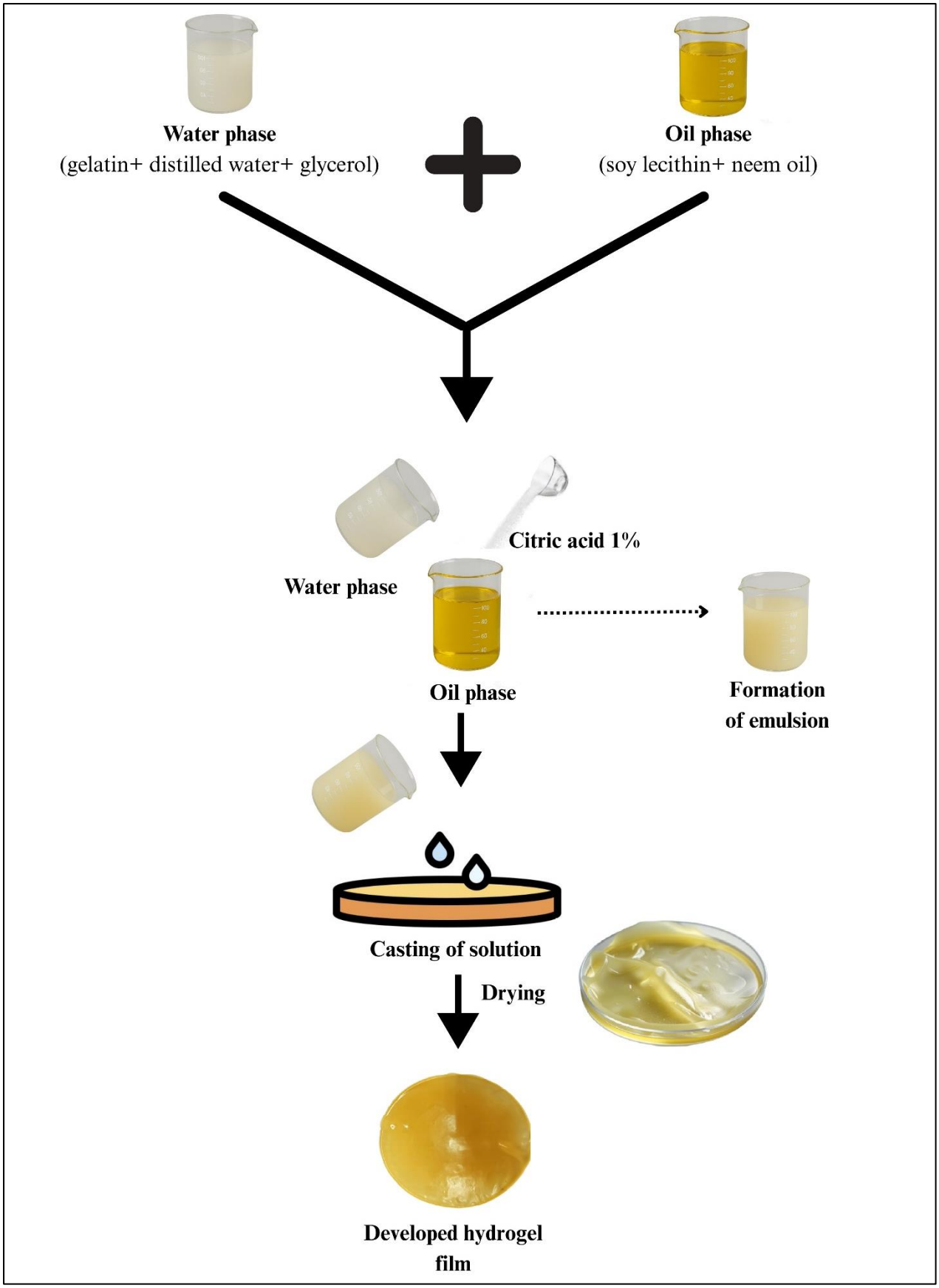
*Values that do not share a common letter are significantly different ($p < 0.05$).

Table 4

Thermal transition characteristics of the selected S2 gelatin-based hydrogel film determined using DSC

Transition	Glass Transition Temperature (Tg, °C)	Onset Temperature (To, °C)	Endset Melt Temperature (Tc, °C)	Melting Peak Temperature (Tm, °C)	Range (Tc – To, °C)	Change in Heat Capacity (ΔCp, $J \cdot g^{-1} \cdot °C^{-1}$)	Enthalpy of Melting (ΔH_m, $J \cdot g^{-1}$)	Peak Height (mW)
First	39.09 (Tg_1)	35.02 (To_1)	43.26 (Tc_1)	—	8.24	0.207 (ΔCp_1)	—	—
Second	51.92 (Tg_2)	185.60 (To_2)	196.92 (Tc_2)	188.70	11.32	0.172 (ΔCp_2)	156.4837	15.4211

*Tg_1, first glass transition temperature; To_1, onset temperature of the first thermal transition; Tc_1, endset melt temperature of the first thermal transition; ΔCp_1, change in heat capacity associated with the first glass transition; Tg_2, second glass transition temperature; To_2, onset temperature of the melting transition; Tc_2, endset melt temperature of the melting transition; ΔCp_2, change in heat capacity associated with the second glass transition; Tm, melting peak temperature; ΔHm, enthalpy of melting; mW, maximum height of the endothermic melting peak.



876

877 **Graphical Abstract:** Development of gelatin-based active biodegradable hydrogel packaging film.